Behavior Research Methods
2010, 42 (4), 1072-1078
doi:10.3758/BRM.42.4.1072

Development of a fully automated system for delivering odors in an MRI environment

Isabel Cuevas, Benoît Gérard, Paula Plaza, Elodie Lerens, and Olivier Collignon
Université Catholique de Louvain, Brussels, Belgium

Cécile Grandin
Cliniques Universitaires St. Luc, Brussels, Belgium

and

Anne G. De Volder and Laurent Renier
Université Catholique de Louvain, Brussels, Belgium

We describe the development and evaluation of a computer-controlled system for delivering odors in a magnetic resonance imaging (MRI) environment. The system allows a timely presentation of different odors in synchrony with MRI sequences and participant's inspiration phase. The rise/fall time of odor deliverance has been optimized to generate prompt and strong stimulations. Equipped with a user-friendly programming interface, the system can be used reliably in a wide range of experimental paradigms. We have paid particular attention to developing a portable system that is relatively easy, rapid, and inexpensive to replicate. The equipment has been tested in a 3-Tesla MRI in a boxcar paradigm, in which stimulation conditions alternated with rest periods (no stimulation). The experiment demonstrated the good functioning of the device and its efficiency in producing the expected activation in the olfactory cortex; it also revealed some methodological and technical aspects to be improved.

Functional magnetic resonance imaging (fMRI) allows the measurement of signal changes related to variations in the brain activity during different perceptual and cognitive tasks (Logothetis, 2008; Matthews & Jezzard, 2004). The magnetic environment hinders the use of any ferrous devices and motivates the development of new methods and equipment to deliver various stimuli in the magnet. Our purposes with the present work were to develop and to test a computer-controlled device able to efficiently and accurately deliver different odors in a timed and reproducible paradigm. The system was tested in a Philips 3-Tesla MRI scanner to probe the neural correlates of olfactory perception.

The air-dilution olfactometer that allows the delivery of chemical stimuli without changing mechanical and thermal conditions in the nasal cavity is the gold standard for clinical applications of chemosensory event-related potentials in neurology and otorhinolaryngology (Rombaux, Mouraux, Bertrand, Guerit, & Hummel, 2006). However, there are other constraints for studying chemosensory processes using electrophysiological methods and brain imaging. For instance, developing an MRI-compatible device requires (1) the use of MRI-compatible elements near the magnet (i.e., without any ferrous metal), (2) timed stimulations, (3) a precise control of the stimulation duration associated with a constant airflow stream to rinse the nasal cavity after each stimulation, (4) prompt rise/fall stimulation times, (5) accurate and reproducible (i.e., with the same intensity) stimulations using various odors, (6) a good resistance to contamination, (7) an automatized computer-control system, and (8) the ability to synchronize the stimulations with fMRI sequences and breathing cycles. Ideally, such system should also have a reliable, flexible, and easy-to-use programming interface that would allow using additional auditory stimulations (e.g., for the instructions) and that would offer the ability to record participants' responses and reaction times. In addition to these requirements, we wanted a system that could be easily and rapidly replicated at a relatively low cost. Although several inexpensive, easy-to-use, and efficient MRI-compatible olfactory stimulators exist (Lorig, Elmes, Zald, & Pardo, 1999; Popp, Sommer, Müller, & Hajak, 2004; Sobel et al., 1997), we wanted to present another system that would constitute a good alternative. The stimulation device we describe here was inspired mainly by the work of Lorig et al. Its characteristics make the present device suitable for a wide variety of experimental paradigms.

Development and Technical Characteristics

Figure 1 shows different views of the system and the arrangement of the valves and lubrificators. The olfactometer is made of a series of nylon, chemically inert, industrial channels and five computer-controlled metallic solenoid valves (24 V_{DC}, 0.19 A, 4.5 W, Norgren). Four of

A. G. De Volder, anne.de.volder@uclouvain.be

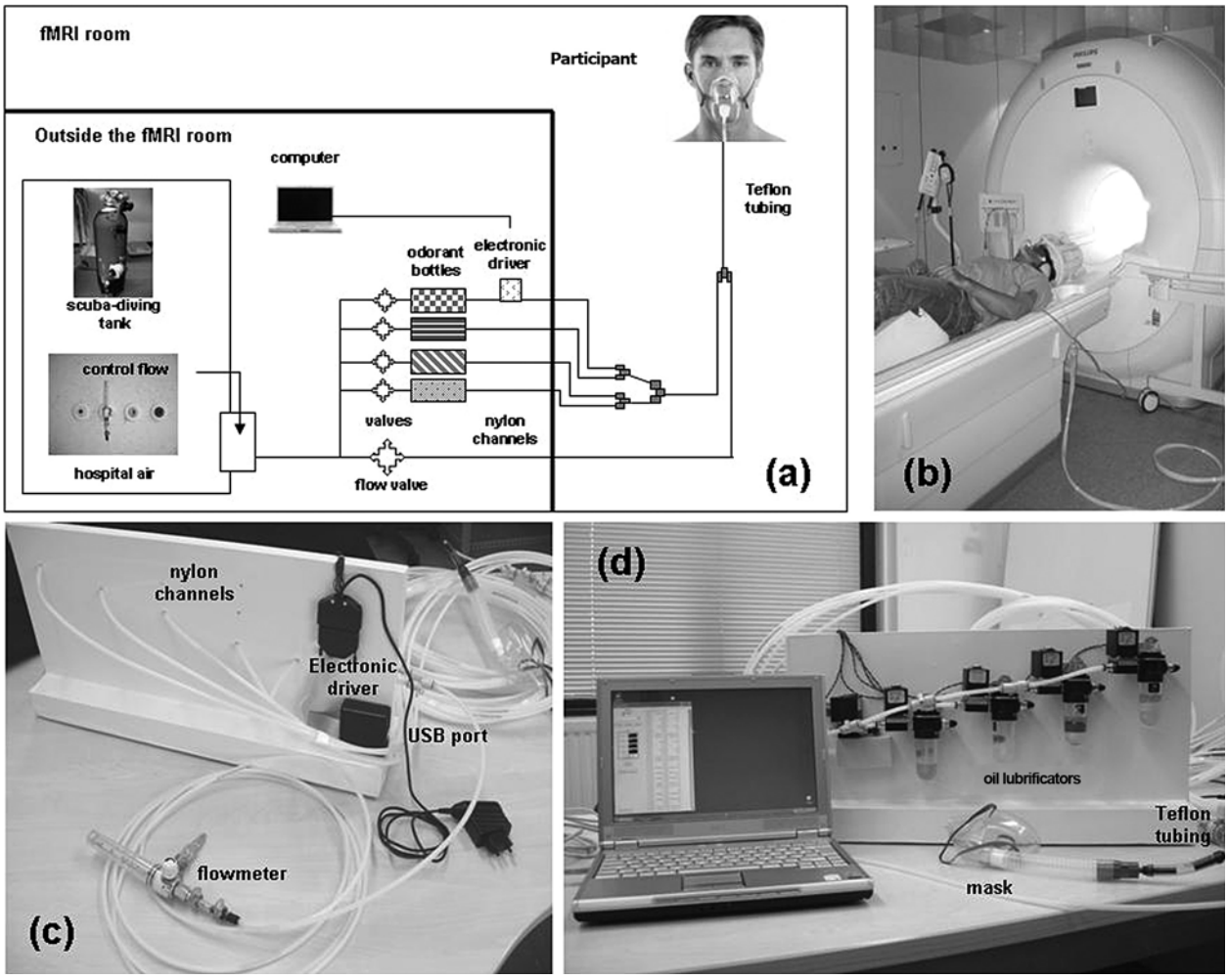

Figure 1. Images of the olfactory stimulator. (A) Schematic representation of the stimulator. Outside and partly inside the fMRI room, the five nylon channels transmit odorless pulsed air and odorants in separate ways, until they reach the last 30-cm segment nearest to the participant; these channels converge into a single Teflon tube connected to a mask. Outside of the fMRI room, compressed air—either from a scuba-diving tank or a hospital air-care delivery (constant flow)—provides a clean air supply for the stimulator. Bottles containing the odorants (lemon, banana, lavender, rose) are kept in the odor delivery system. An electronic driver is located in the back of the stimulator device (represented schematically in the figure). The computer that controls the stimulator device is located outside the fMRI room. (B) Image of a volunteer participating in an experiment using the stimulator in the MRI scanner. Auditory signals that allow synchronization of breathing with odor stimulations are delivered via headphones. (C, D) Overall view of the computer-controlled stimulator device, showing nylon channels, fittings, and Teflon tube that deliver the switched air streams to the participant via a removable medical mask; panel C shows the view from the back, showing the flowmeter, the start of the five nylon channels, the main power, and the electronic driver, which is equipped with a USB port; panel D gives a detailed front view of the device, showing the solenoid valves and oil lubrificators containing the odors in solution. The main part of the device and the computer remain outside the fMRI room, whereas the five nylon channels are passed to the fMRI room through a conventional security hole.

these channels are connected to a separate miniaturized oil lubrificator (Norgren) that contains a distinct odorant in solution. At the output of the flow valves, four nylon channels allow the separate delivery of different odors. The fifth solenoid valve is connected to an air-stream control channel that pulses air directly into the last segment of the stream. The length of the five channels can be adapted according to the configuration of the MRI room. Near to the participant, the channels are subsequently connected 2×2 through five nylon three-way connecting tubes, with the control air stream connected as the last one, to converge to a single 30-cm Teflon tube (diameter: 4 mm) that delivers the switched air streams to the participant via a medical respiratory mask. The five nylon channels are attached together with plastic rings, since this is the only part of the device that is manually inserted through the fMRI wall security hole to reach the magnet. Outside of the fMRI room, compressed air, either from a scuba-diving tank (capacity, 3 m^3) or from the hospital air-care delivery, provides clean air supply for the stimulator at a pressure of 5 bars. A flow valve limits the airflow entering the system via a single nylon channel (see Figure 1). The flow valve chosen for this application was a direct-reading 150-mm glass-float medical oxygen flush device (15 l/min) with built-in flow indicator (Ohmeda). This medical oxygen flush device could be replaced by any factory-calibrated

flow valve that offers an equivalent accuracy. Each part of the system can resist a pressure exceeding 10 bars. The lubrificators were carefully cleaned with soap in solution and rinsed in water before the first use. Bacteriological safety is assured by cleaning the removable medical mask with detergent and conventional isopropyl alcohol disinfectant between each fMRI acquisition. Although nylon channels were used in the present study, Teflon or any other low odor-absorbing material may be more appropriate, since nylon may retain odors after several uses.

The solenoid valves are operated by a computer-controlled 12-VCD relay driver and by digital relays on a USB port (National Instruments). During control operation (no stimulation), air supply does not enter the odor channels, all four solenoids being turned off. It enters only the control solenoid, which is turned on, passes through the nylon control channel, and is further transmitted into the 30-cm Teflon tubing connected to the participant. In order to eliminate residual odors, airflow is constantly delivered to the participant during control conditions. One second before the intended stimulation, one of the four solenoids is turned on and the control solenoid is automatically turned off. This stops the control flow, and the selected odor is then transmitted through the corresponding nylon channel to the participant via the Teflon tubing and the mask. The airflow characteristics (i.e., strength and temperature) of the control flow are identical to those of the odor flow, so there is no mechanical or thermal change at the beginning or at the end of the stimulation. Pretests performed with 5 participants confirmed that, with an airflow of 15 l/min, olfactory stimulations were efficient and accurate and remained comfortable for the participant; the rise time to detect an odor was about 1 sec, enough time to eliminate any odor from the tubes. With such air outflow (15 l/min), participants perceived a constant somatosensory stimulation on their face during both olfactory stimulation and no stimulation conditions. However, a habituation to the airflow stimulation rapidly occurred, and participants became unaware of it after a few minutes.

The solenoids (and hence the air and odor flows) are controlled by a computer interface using a remote-control program (task manager) implemented in LabVIEW software. Although the solenoid valves, the lubrificators, the relay driver used for electronic interface, and the control computer are located outside the fMRI room, only the air tubes and the mask are positioned near the magnet. Via the control computer, the odor delivery system can be manipulated interactively, or a prepared script can be launched by a dedicated program in LabVIEW. For fMRI, a script file is implemented, which allows audio files to be uploaded and sent to the participants through headphones, with a predefined timing sequence (see below). Prior to each first brain volume of active conditions, the fMRI system sends a trigger pulse to the control computer. In the script, an electronic feedback loop controls the proper interpretation of each trigger pulse in the fMRI paradigm, ensuring that there is no time shift between data acquisition and odor delivery. Although the participants were not required to provide any response during the present experiment, the system offers the ability to record participants' responses (e.g., odor or no odor) via a response button pad. Reaction times corresponding to these responses could be calculated throughout the experiment if desired.

Evaluation of the Olfactory Stimulator: Operational fMRI Example

Participants. The study was carried out with 2 male volunteers (ages 21 and 24 years), who were blindfolded during the different phases of the experiment. Participants were healthy, were right handed (as assessed with the Edinburg handedness inventory; Oldfield, 1971), and gave written informed consent beforehand. To ensure normal olfactory function, we tested participants with the Sniffin' Sticks Test (Burghart Medical Technology; Hummel, Kobal, Gudziol, & Mackay-Sim, 2007; Hummel, Sekinger, Wolf, Pauli, & Kobal, 1997; Kobal et al., 2000), and all performed within the normal range. The experimental protocol was approved by the Biomedical Ethics Committee of the School of Medicine of the Université Catholique de Louvain.

Experimental setup and stimuli. Four chemical odorants (Sigma Aldrich, Germany) were used in the odor delivery system for this experiment: lemon (3,7-Dimethyl-2,6-octadienal), banana (Isoamyl acetate), lavender (1-Octen-3-yl acetate), and rose (2-Phenyl ethyl alcohol). Odorants were diluted to a concentration of 10% using mineral oil (Sigma Aldrich, Germany), and 5 ml of each odorous solution was prepared. A timed stimulation paradigm was created to allow olfactory stimulations to be synchronized with the inspiration phase, using auditory signals (described in the following section). An MRI-compatible, high-definition piezoelectric sound delivery system was used (the so-called SDS device; the fMRI.pl group, www.fmri.pl). These headphones provided the participants with good acoustic isolation to protect their ears from MRI scanner noise. Participants could, therefore, hear no noise from the olfactory stimulator. We used auditory signals—a high-frequency (264-Hz) and a low-frequency (132-Hz) pure tone of about 860 msec each—to inform the participant when to breathe in and when to breathe out.

Experimental paradigm and procedures. In the present study, we used a block design paradigm with periods of passive olfactory stimulation (odor condition, O) alternating with periods without any olfactory stimulation (no-odor condition, NO), during which participants received odorless pulsed air. The choice of the block design paradigm and of the duration of the epoch was mostly arbitrary in the present study, and other designs, such as event-related design, could also work.

The fMRI paradigm consisted of four runs of seven alternating epochs of O and NO conditions (30 sec per active epoch, corresponding to 10 brain volumes). Six stimuli were presented during each O condition, and the olfactory stimuli (lemon, lavender, banana, and rose) were presented pseudorandomly. Although six stimulations were delivered during one epoch for a breathing cycle of 6 sec, with a 2/1 expiration/inspiration ratio, the processing of only the five first stimulations probably took place during the epoch (the processing of the sixth being very close to the end of the epoch).

Participants had to control their breathing according to auditory signals transmitted through headphones during both O and NO conditions. To synchronize the stimulations with the inspirations, the olfactory stimulations were sent at the end of the expiration to ensure that the participants inhaled the odorant, as was recommended by Vigouroux, Bertrand, Farget, Plailly, and Royet (2005). Each trial began when the auditory signal for the expiration was delivered through the headphones. Three seconds after the expiration signal, the intended solenoid for odorant delivery was turned on; 1 sec later, the participant started inhaling (see Figure 2). At the next expiration signal—2 sec after the beginning of the inspiration—the odorant solenoid was turned off, and the control solenoid was automatically turned on to flush out the residual odors with clean air during the expiration phase.

The use of relatively brief stimulations (2 sec) limited the risk of adaptation to the odors. In addition, to attenuate any potential habituation phenomenon, different odors alternated in a same epoch. Each run was separated by a 5-min break, as was recommended by Poellinger et al. (2001).

Training. Before the MRI experiment, two 1-h sessions were devoted to train participants to adopt a breathing cycle of 6 sec, according to the auditory signals (see the Experimental Set-up and Stimuli section above). This training phase also aimed secondarily to familiarize participants with the experimental conditions. In the present experiment, we used the same odorants as those used in the fMRI study, but such familiarization could be done with other odors—or even without any olfactory stimulation—to avoid any potential habituation to the stimuli. Participants were required to listen carefully to each auditory signal and to control their breathing, as instructed. Odorants and odorless airflow were delivered pseudorandomly. At the end of the familiarization sessions, the participants were able to control their breathing cycle, using the auditory signals, and to adopt a breathing cycle of 6 sec (4 sec for expiration, 2 sec for inspiration). All participants reported having detected the odorants at the very first period of stimulation.

Data acquisition and processing. Structural brain imaging was obtained in the 2 participants in the bicommissural orientation (anterior and posterior commissure [AC–PC]; Talairach & Tournoux, 1988) on a 3-Tesla MRI scanner (Achieva, Philips Medical systems) using a 3-D fast T1-weighted gradient echo sequence with an inversion prepulse (Turbo field echo [TFE], TR [repetition time] = 9 msec, TE [echo time] = 4.6 msec, flip angle = 8°, 150 slices, 1-mm thickness, in-plane resolution = 0.81 × 0.95 mm). The field of view was 220 × 197 mm, and the sense factor (parallel imaging) was 1.5. We used

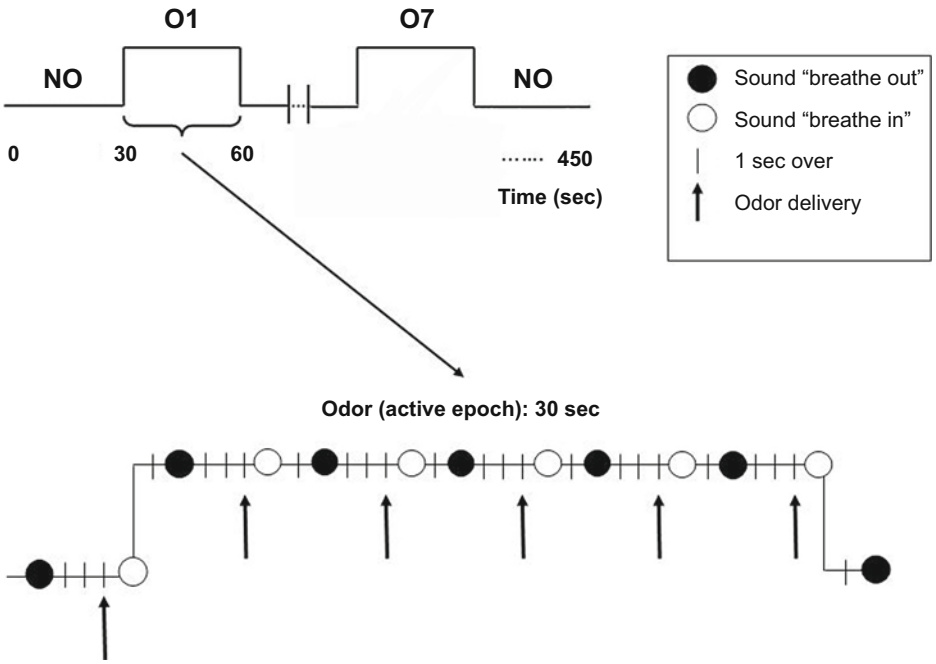

Figure 2. Experimental paradigm used in the present study. The paradigm consisted of a block design with passive olfactory stimulation periods (odor [O] condition) alternating with resting periods exempt of olfactory stimulations (no-odor [NO] condition). Each active epoch lasted for 30 sec, during which time six odors were delivered to the participant. The paradigm consisted of four runs of seven alternating epochs (O1–O7). The two perpendicular lines in the intermediate NO condition indicate that several other blocks were used. The arrows indicate when the odors were delivered, which coincides with the beginning of the participant's inspiration phases. The circles indicate when the auditory signals were sent: The plain (black) circles correspond to the expiration phases and the empty (white) circles to the inspiration phases. Participants had to control their breathing rhythm during both O and NO conditions. Each trial began during an expiration phase (plain black circle). Three seconds after the beginning of the expiration, the first odorant was delivered (black arrow); 1 sec later, the participant received the inspiration auditory signal.

an eight-channel phased-array head coil. Foam pads restrained each participant's head throughout the study.

BOLD fMRI data were acquired using a 2-D simple-shot, T2-weighted gradient echo-planar imaging (EPI) sequence (TR = 3,000 msec, TE = 27 msec), with 48 axial slices (slice thickness = 2.4 mm) in the AC–PC orientation. The matrix was 112 × 112 × 44, the field of view was 220 mm^2, and in-plane resolution was 2.12 mm.

Data were processed and analyzed using Statistical Parametric Mapping (SPM 2, Wellcome Department of Imaging Neuroscience, London; www.fil.ion.ac.uk/spm), which was implemented in MATLAB (The MathWorks, Inc., Natick, MA). The first 10 volumes of each run were discarded to allow for T1 equilibration and participant relaxation. The individual structural (TFE) brain volume was coregistered to the first remaining fMRI volume of the corresponding participant. The 3-D structural volume was then spatially normalized into the referential defined by the Talairach and Tournoux (1988) atlas and by the MRI template supplied by the Montreal Neurological Institute (MNI). The fMRI data were spatially realigned, using a trilinear interpolation (Friston et al., 1995) and were further spatially normalized using the normalization parameters derived from the 3-D structural (TFE) normalization, resulting in normalized fMRI scans with a cubic voxel size (2 × 2 × 2 mm) for individual analysis. Next, a spatial smoothing with a Gaussian kernel of 6 mm (full width at half maximum) was applied.

We estimated condition-related changes in regional brain activity for each participant, using a general linear model in which the responses evoked by each condition of interest were modeled by a standard hemodynamic response function. To identify the cerebral regions significantly activated by the olfactory stimulations, we computed the contrast of interest at the individual level, with the statistical threshold set at $p < .001$ (uncorrected) and extending to at least 20 contiguous voxels.

Results

In Participant 1, the contrast (O − NO) was associated with brain activation in frontal brain areas including the left orbitofrontal cortex (BA 11/47). Another brain activation focus was found between the posterior part of the piriform cortex and the amygdala, with coordinates (−20, −2, −16; see Table 1 and Figure 3). In Participant 2, this contrast also showed brain activation in the frontal brain areas, including the left orbitofrontal cortex (BA 11). Another brain activation focus was observed in the limbic lobe with coordinates (−18, −2, −20), including the left anterior entorhinal cortex (BA 34), the amygdala, and the

Table 1
Overview of Activation Foci Obtained in the Experimental Condition (i.e., Using the Contrast "Odor − No Odor" in Participants 1 and 2)

Brain Area	Brodmann Area	Side	Cluster Size	*Z* Score	Coordinates (mm)		
					x	*y*	*z*
Participant 1							
Inferior frontal gyrus	BA 46	R	280	5.20	48	42	10
Middle frontal gyrus	BA 10	R	–	4.74	42	54	10
Inferior frontal gyrus	BA 46	R	–	4.62	40	42	6
Orbital gyrus	BA 11	R	59	4.74	18	64	−12
Superior frontal gyrus	BA 11	R	–	4.40	20	56	−10
Middle frontal gyrus	BA 11/47	L	84	4.69	−36	36	−10
Orbitofrontal cortex							
Middle frontal gyrus	BA 11	L	32	4.59	−24	38	−12
Orbitofrontal cortex							
Inferior temporal gyrus	BA 20	L	28	3.93	−54	−12	−38
Piriform cortex/amygdala	–	L	41	3.85	−20	2	−16
Middle frontal gyrus	BA 10	L	24	3.47	−46	50	4
Participant 2							
Cerebellum	–	R	8,091	12.66	28	−84	−26
Cerebellum	–	L	–	11.80	−28	−76	−26
Cerebellum	–	L	–	11.79	−40	−76	−26
Superior temporal gyrus	BA 38	L	415	10.70	−22	10	−32
Inferior parietal lobule	BA 40	R	2,890	10.54	38	−34	42
Middle frontal gyrus	BA 10	L	1,512	7.54	−46	54	−4
Superior frontal gyrus	BA 11	L	348	8.30	−22	42	−20
Orbitofrontal cortex							
Superior frontal gyrus	BA 10	L	–	7.78	−22	58	−4
Middle frontal gyrus	BA 10	L	62	5.58	−40	42	22
Limbic lobe	BA 34	L	50	5.33	−18	−2	−20
Entorhinal cortex/amygdala							
Piriform cortex/amygdala	–	L	–	4.56	−20	2	−16
Middle occipital gyrus	BA 19	L	85	5.19	−24	−98	14
Middle temporal gyrus	BA 22	L	113	5.10	−50	−36	−8
Cuneus	BA 17	L	161	3.47	0	−92	4

Note—Coordinates are reported in MNI space, as given by SPM2, and correspond only approximately to Talairach and Tournoux space (Talairach & Tournoux, 1988). BA, Brodmann area; $p < .001$, uncorrected for multiple comparisons. R, right; L, left.

left piriform cortex. Additional brain activation foci were observed in the cerebellum (bilaterally) and in temporal, parietal, and occipital brain areas (see Table 1).

Discussion

In the present article, we have described an automated system for delivering odors in an MRI environment. The system was relatively inexpensive, was easy to develop, and demonstrated its reliability and efficiency to activate most regions in the olfactory cortex. The present system allows synchronizing the olfactory stimulations with the inspiration phases of the participant, which is crucial to optimize olfactory activation and to allow controlling activations related to sniffing (Simonyan, Saad, Loucks, Poletto, & Ludlow, 2007; Sobel et al., 1998). However, constraining participants to adopt a novel breathing rhythm may appear problematic for some and may interfere with the realization of cognitive tasks. In addition, this method induces auditory and attention-related brain activation that could interfere differently with the brain activity during the O and NO conditions. Another weakness of our method is that it does not allow controlling the inspiration amplitude, which may influence the activation. Other methodological and technical aspects could also be improved. Although our equipment did not seem to have absorbed any odor, in the long term, Teflon tubing may be more appropriate than nylon channels are for conveying odorants. In any case, the equipment should be inspected thoroughly after each use, to ensure that no part of the equipment has retained any odor. In the present study, we used the same stimuli during the training sessions and during the fMRI experiment, which may have induced a habituation to the odors and, therefore, reduced olfactory activation. Ideally, different odors should be used to prevent this problem. Finally, the last stimulus (the sixth one) in each O condition was too close to the end of the epoch and may have contaminated a small portion of the NO conditions. Ideally, we should have either deleted the last stimuli or extended a little bit the duration of the epoch. The event-related design is also a good alternative to the block-design paradigm.

The evaluation of the system in 2 participants demonstrated its efficiency to produce robust brain activation, similar to those observed in studies using other olfactory stimulators (Popp et al., 2004; Sobel et al., 1997; Vigouroux et al., 2005; Zald & Pardo, 2000). In accordance with previous studies that used passive olfactory stimulation (Boyle, Frasnelli, Gerber, Heinke, & Hummel, 2007; Savic & Berglund, 2004; Savic, Gulyas, Larsson, & Roland, 2000; Zatorre, Jones-Gotman, Evans, & Meyer, 1992) as well as more complex chemosensory tasks (Plailly et al., 2005; Royet et al., 1999; Sobel et al., 2000), brain activation foci were found mainly in frontal brain areas, including the orbitofrontal, entorhinal, and piriform cortices, and the amygdala. The insula was not activated in the present study, although this structure is known to be part of the olfactory network (Royet & Plailly, 2004; Zald & Pardo, 2000) and is usually recruited during passive smelling of odors and discrimination of odor quality (Savic et al., 2000). However, the small size of the sample may account for this difference. The relatively weak recruitment of the amygdala in Participant 1 may be due to the fact that pleasant odors were used (rose, lavender, banana, lemon) and this brain structure is usually specifically activated when unpleasant or aversive odors are perceived (Gottfried, Deichmann, Winston, & Dolan, 2002; Zald & Pardo, 1997). In the present study, Participant 2 showed activation in the occipital cortex (mainly BA 19 bilaterally). Interestingly, previous studies using PET and

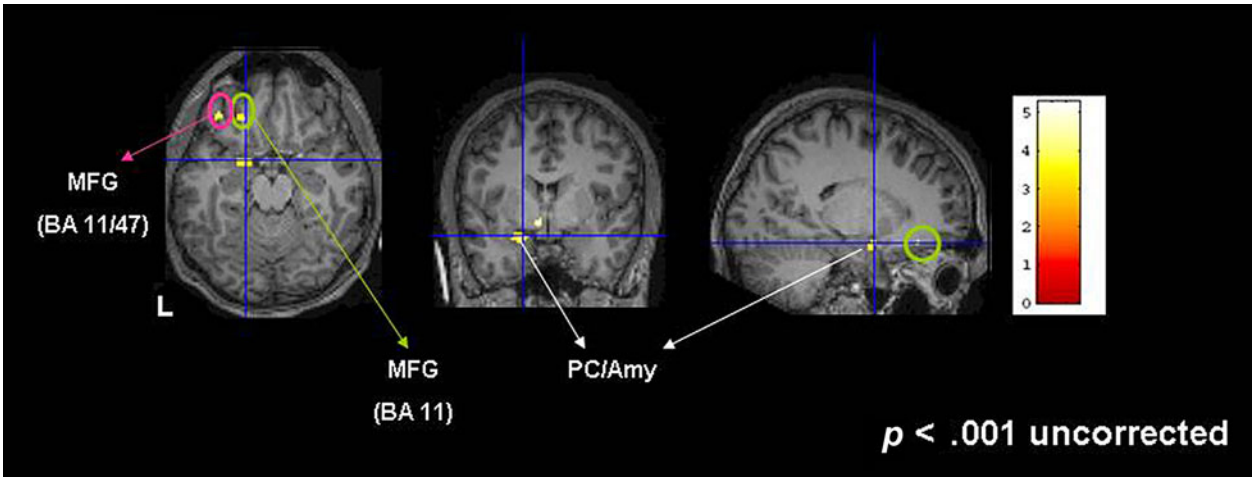

Figure 3. Brain activation patterns observed in one of the two volunteers during passive chemosensory stimulations: odor (O) conditions − no-odor (NO) conditions. The statistical parametric maps for this comparison are superimposed on the axial, coronal, and sagittal sections of the individual normalized MRI. Only positive differences exceeding a threshold of $p < .001$ (uncorrected) are shown, according to the color scales, which code the *T* values. The lines intersect at coordinates ($x, y, z = -20, -2, -16$), in a brain-activation focus located between the posterior part of the piriform cortex (PC) and the amygdala (Amy; Boyle, Frasnelli, Gerber, Heinke, & Hummel, 2007), with a *Z* value of 3.85. The green circle indicates a focus in the left middle frontal gyrus (MFG; BA 11) in and around the left orbitofrontal cortex. The pink circle indicates a focus in the left MFG (BA 11/47) corresponding to the left orbitofrontal cortex. L = left side of the brain.

fMRI in sighted participants showed similar brain activation in the occipital cortex during odor identification (Suzuki et al., 2001), in odor naming (Qureshy et al., 2000), and in hedonicity, edibility, and familiarity judgments (Plailly et al., 2005; Royet et al., 2001). This activation in the occipital cortex was interpreted as the recruitment of visual imagery processes triggered by the perception of odors (Qureshy et al., 2000; Royet et al., 2001).

In conclusion, although other systems that are equally efficient and technically equivalent to ours have been proposed, the present system represents a good alternative for researchers who want to develop a reliable MRI-compatible olfactory stimulator.

AUTHOR NOTE

We thank the Fonds Special de Coopération Universitaire au Développement for supporting I.C. and P.P. We also thank P. Rombaux for his helpful comments on the manuscript. A.G.D.V. is senior research associate and L.R. and O.C. are postdoctoral researchers at the National Funds for Scientific Research (Belgium). This study was supported by FRSM Grant 3.4502.08 (Belgium). Address correspondence to A. G. De Volder, Avenue Hippocrate, 54, UCL-54.46, B-1200 Brussels, Belgium (e-mail: anne.de.volder@uclouvain.be).

REFERENCES

Boyle, J. A., Frasnelli, J., Gerber, J., Heinke, M., & Hummel, T. (2007). Cross-modal integration of intranasal stimuli: A functional magnetic resonance imaging study. *Neuroscience*, **149**, 223-231. doi:10.1016/j.neuroscience.2007.06.045

Friston, K. J., Holmes, A. P., Worsley, K. J., Poline, J.-P., Frith, C. D., & Frackowiak, R. S. J. (1995). Statistical parametric maps in functional imaging: A general linear approach. *Human Brain Mapping*, **2**, 189-210.

Gottfried, J. A., Deichmann, R., Winston, J. S., & Dolan, R. J. (2002). Functional heterogeneity in human olfactory cortex: An event-related functional magnetic resonance imaging (fMRI) study. *Journal of Neuroscience*, **22**, 10819-10828.

Hummel, T., Kobal, G., Gudziol, H., & Mackay-Sim, A. (2007). Normative data for the "Sniffin' Sticks" including tests of odor identification, odor discrimination, and olfactory thresholds: An upgrade based on a group of more than 3,000 subjects. *European Archives of Oto-rhino-laryngology*, **264**, 237-243. doi:10.1007/s00405-006-0173-0

Hummel, T., Sekinger, B., Wolf, S. R., Pauli, E., & Kobal, G. (1997). "Sniffin' Sticks": Olfactory performance assessed by the combined testing of odor identification, odor discrimination, and olfactory threshold. *Chemical Senses*, **22**, 39-52. doi:10.1093/chemse/22.1.39

Kobal, G., Klimek, L., Wolfensberger, M., Gudziol, H., Temmel, A., Owen, C. M., et al. (2000). Multicenter investigation of 1,036 subjects using a standardized method for the assessment of olfactory function combining tests of odor identification, odor discrimination, and olfactory thresholds. *European Archives of Oto-rhino-laryngology*, **257**, 205-211. doi:10.1007/s004050050223

Logothetis, N. K. (2008). What we can do and what we cannot do with fMRI. *Nature*, **453**, 869-878. doi:10.1038/nature06976

Lorig, T. S., Elmes, D. G., Zald, D. H., & Pardo, J. V. (1999). A computer-controlled olfactometer for fMRI and electrophysiological studies of olfaction. *Behavior Research Methods, Instruments, & Computers*, **31**, 370-375.

Matthews, P. M., & Jezzard, P. (2004). Functional magnetic resonance imaging. *Journal of Neurology, Neurosurgery, & Psychiatry*, **75**, 6-12.

Oldfield, R. C. (1971). The assessment and analysis of handedness: The Edinburgh inventory. *Neuropsychologia*, **9**, 97-113. doi:10.1016/0028-3932(71)90067-4

Plailly, J., Bensafi, M., Pachot-Clouard, M., Delon-Martin, C., Kareken, D. A., Rouby, C., et al. (2005). Involvement of right piriform cortex in olfactory familiarity judgements. *NeuroImage*, **24**, 1032-1041. doi:10.1016/j.neuroimage.2004.10.028

Poellinger, A., Thomas, R., Lio, P., Lee, A., Makris, N., Rosen, B. R., & Kwong, K. K. (2001). Activation and habituation in olfaction—An fMRI study. *NeuroImage*, **13**, 547-560. doi:10.1006/nimg.2000.0713

Popp, R., Sommer, M., Müller, J., & Hajak, G. (2004). Olfactometry in fMRI studies: Odor presentation using nasal continuous positive airway pressure. *Acta Neurobiologiae Experimentalis*, **64**, 171-176.

Qureshy, A., Kawashima, R., Imran, M. B., Sugiura, M., Goto, R., Okada, K., et al. (2000). Functional mapping of human brain in olfactory processing: A PET study. *Journal of Neurophysiology*, **84**, 1656-1666.

Rombaux, P., Mouraux, A., Bertrand, B., Guerit, J. M., & Hummel, T. (2006). Assessment of olfactory and trigeminal function using chemosensory event-related potentials. *Clinical Neurophysiology*, **36**, 53-62. doi:10.1016/j.neucli.2006.03.005

Royet, J.-P., Hudry, J., Zald, D. H., Godinot, D., Grégoire, M. C., Lavenne, F., et al. (2001). Functional neuroanatomy of different olfactory judgments. *NeuroImage*, **13**, 506-519. doi:10.1006/nimg.2000.0704

Royet, J.-P., Koenig, O., Grégoire, M. C., Cinotti, L., Lavenne, F., Le Bars, D., et al. (1999). Functional anatomy of perceptual and semantic processing for odors. *Journal of Cognitive Neuroscience*, **11**, 94-109. doi:10.1162/089892999563166

Royet, J.-P., & Plailly, J. (2004). Lateralization of olfactory processes. *Chemical Senses*, **29**, 731-745. doi:10.1093/chemse/bjh067

Savic, I., & Berglund, H. (2004). Passive perception of odors and semantic circuits. *Human Brain Mapping*, **21**, 271-278. doi:10.1002/hbm.20009

Savic, I., Gulyas, B., Larsson, M., & Roland, P. (2000). Olfactory functions are mediated by parallel and hierarchical processing. *Neuron*, **26**, 735-745. doi:10.1016/S0896-6273(00)81209-X

Simonyan, K., Saad, Z. S., Loucks, T. M. J., Poletto, C. J., & Ludlow, C. L. (2007). Functional neuroanatomy of human voluntary cough and sniff production. *NeuroImage*, **37**, 401-409. doi:10.1016/j.neuroimage.2007.05.021

Sobel, N., Prabhakaran, V., Desmond, J. E., Glover, G. H., Goode, R. L., Sullivan, E. V., & Gabrieli, J. D. E. (1997). A method for functional magnetic resonance imaging of olfaction. *Journal of Neuroscience Methods*, **78**, 115-123. doi:10.1016/S0165-0270(97)00140-4

Sobel, N., Prabhakaran, V., Desmond, J. E., Glover, G. H., Goode, R. L., Sullivan, E. V., & Gabrieli, J. D. E. (1998). Sniffing and smelling: Separate subsystems in the human olfactory cortex. *Nature*, **392**, 282-286.

Sobel, N., Prabhakaran, V., Zhao, Z., Desmond, J. E., Glover, G. H., Sullivan, E. V., & Gabrieli, J. D. E. (2000). Time course of odorant-induced activation in the human primary olfactory cortex. *Journal of Neurophysiology*, **83**, 537-551.

Suzuki, Y., Critchley, H. D., Suckling, J., Fukuda, R., Williams, S. C. R., Andrew, C., et al. (2001). Functional magnetic resonance imaging of odor identification: The effect of aging. *Journals of Gerontology*, **56A**, M756-M760.

Talairach, J., & Tournoux, P. (1988). *Co-planar stereotaxic atlas of the human brain*. New York: Thieme.

Vigouroux, M., Bertrand, B., Farget, V., Plailly, J., & Royet, J.-P. (2005). A stimulation method using odors suitable for PET and fMRI studies with recording of physiological and behavioral signals. *Journal of Neuroscience Methods*, **142**, 35-44. doi:10.1016/j.jneumeth.2004.07.010

Zald, D. H., & Pardo, J. V. (1997). Emotion, olfaction, and the human amygdala: Amygdala activation during aversive olfactory stimulation. *Proceedings of the National Academy of Sciences*, **94**, 4119-4124. doi:10.1073/pnas.94.8.4119

Zald, D. H., & Pardo, J. V. (2000). Functional neuroimaging of the olfactory system in humans. *International Journal of Psychophysiology*, **36**, 165-181. doi:10.1016/S0167-8760(99)00110-5

Zatorre, R. J., Jones-Gotman, M., Evans, A. C., & Meyer, E. (1992). Functional localization and lateralization of human olfactory cortex. *Nature*, **360**, 339-340. doi:10.1038/360339a0

(Manuscript received December 2, 2009;
revision accepted for publication May 17, 2010.)